Lunds universitet
Lunds Tekniska Högskola

Characterisation of Drained Properties of Swedish Clay Till

Yohanes Armediaz

November 2023
Lund University

Svenska Byggbranschens Utvecklingsfond

Trafikverket

Acknowledgements

The research project has been jointly financed by Svenska byggbranschens utvecklingsfond (SBUF) and Branschsamverkan i grunden (BIG).

The author would like to express his deepest appreciation to his supervisors, Erika Tudisco, Minna Karstunen and Per Lindh, who have willingly spent their time to provide invaluable help to the project, without which the project would not be feasible.

The author would like to thank members of the reference group for providing guidance and assistance to the project. The members of the reference group are:

- Nils Rydén — PEAB-LTH
- Kristy Heng — Trafikverket
- Daniel Baltrock — C3S Miljoteknik (previously PEAB)
- Anders Emanuelsson — NCC (replacing Lars Nilsson)
- Sven Liedberg — SKANSKA
- Mats Svensson — Tyréns
- Ann Dueck — Claytech
- Henrik Möller — Henrik Möller Geokonsult AB

The author would also like to show his gratitude to people outside the reference group (Martin Holmén from SGI, Magnus Palm from Tyréns, Håkan Lindgren from Sweco) who have also provided inputs into the project which has helped immensely.

Yohanes Armediaz, Lund, November 2023

Contents

1 Introduction

1.1 Motivation

Demand for crucial infrastructures in Skåne has increased recently due to population and economic growth. However, construction can prove troublesome due to the unpredictable behaviour of clay till which is the majority of the underlying soil in the region and also to Copenhagen. Clay till is a type of till, an unsorted glacial sediment, with a clay content between 15% to 50%. While this type of soil is known to be stiff, as infrastructure grows to accommodate the growing population, there is a growing need to know its limit. Furthermore, clay is highly heterogeneous which will greatly vary its strength depending on its location.

At present, drained properties of clay till is determined empirically. However, effective stress parameters is expected to be the governing situation for clay till with less clay content between 15% and 17% (Hartlén, 1974). Design based on the current empirical analysis can then be potentially ineffective in terms of cost and material if the assumption underestimate the drained properties. This is supported by the feedback of the industry that indeed clay till is expected to be stiffer than the values obtained from the empirical relatinship. Thus, to support a more climate-friendly construction moving forward in terms of raw materials usage, there will be a need to have a better understanding of behaviour of clay till.

While there have been various studies carried out on clay till, they have mostly been focusing on the undrained properties. The drained properties are then derived empirically or assumed from the undrained properties. This can lead to a very conservative geotechnical design with consequent unnecessary economic and environmental costs. Therefore, there is a need to perform a thorough research on the drained properties on clay till in order to optimise the geotechnical design used in the industry.

1.2 Aim & Objectives

In this project, an experimental investigation campaign to study the drained properties of clay till found in Skåne is conducted.

This campaign first identified a suitable site where clay till can be found. Then, both in-situ tests and sample collection were performed, after which laboratory tests were conducted. Additionally, imaging analysis were performed to analyse the sample to identify how the inclusions are affecting the behaviour of the soil under shearing. Last, but not least, the results obtained were used as a benchmark and compared to empirical formula currently used in the industry to determine if the current empirical relationship is sufficient or if there is a need to further improve it.

1.3 Limitations

Due to limited resources, only one site was used for the in-situ field test and sample collection. Additionally, due to difficulty in obtaining undisturbed clay till samples, remoulded samples were used for the laboratory tests. While doing so does not give a representative results of the material properties that is found in the site, a known stress history of the sample will be available. This allows a more accurate analysis for modelling purposes in terms of determining the intrinsic properties of the material.

1.4 Organisation of report

The organisation of the report will be as follows:

- Chapter 1 - Introduction
  The general background and current issues has been described. The objectives and the scope have also been established.

- Chapter 2 - Literature Review
  An analysis of past works that have been performed on drained properties of clay till will be presented.

- Chapter 3 - Experimental Campaign
  A description of the experimental campaign, from the selection of the site and the proposed tests to be conducted, will be presented.

- Chapter 4 - Triaxial Test Setup
  The triaxial test setup which was used in this project will be described.

- Chapter 5 - Results
  Results from the tests conducted will be highlighted here.

- Chapter 6 - Imaging Analysis
  A background of imaging analysis alongside with the tests done so far in this project will be presented

- Chapter 7 - Discussions
  Discussions on the results thus far obtained in this project will be discussed here.

- Chapter 8 - Conclusion & Recommendations
  A summary of the project will be highlighted here including proposals and recommendations moving forward.

2

LITERATURE REVIEW

This chapter sets out to outline what is currently known about the drained properties of clay till. This includes past research both in Sweden and neighbouring countries such as Denmark. This will form as the basis for this project so as to determine what is needed to be further investigated.

2.1 Past Research on Clay Till

In Sweden, one of the earliest research on the drained properties of clay till was conducted in the 70's (Hartlén, 1974). In this report, the author looked into the strength and load bearing capacity of clay till. This was done by performing both field tests and laboratory tests. Six sites located in southwestern Sweden were chosen with different types of clay till. The key finding from the research includes equations to approximate both the undrained (undrained shear strength, τ_{fu}) and drained (effective cohesion, c', and friction angle, ϕ') mechanical properties using the initial water content w_0, void ratio e_0 and clay content l, see Equation 2.1 to 2.4. However, it is important to note that the equations obtained in this study were obtained empirically using multiple regression analyses. This could potentially means that these equations could only be valid for the 6 sites studied.

$$c_u = 18 * w_0^{-2.05} * e_0^{-1.88} * l_c^{2.66)} \quad c_u \leqslant 200kPa \tag{2.1}$$

$$c' = 3 * w_0^{-3.23} * e_0^{-2.12} * l_c^{4.19} \quad ifc' \leqslant 20kPa \tag{2.2}$$

$$c' = -24 - 140 * logw_0 - 80.9 * loge_0 + 155 * logl_c \quad if20kPa \leqslant c' \leqslant 50kPa \tag{2.3}$$

$$\phi' = 22 * w_0^{0.166} * e_0^{-0.139} * l_c^{-0.311} \quad 24^\circ \leqslant \phi' \leqslant 33^\circ \tag{2.4}$$

Alternatively, another study on the drained properties on clay till was also conducted in Denmark at the same time frame (Jacobsen, 1970). Similar to (Hartlén, 1974), field and laboratory tests were conducted, this time on 7 sites in Denmark. The author proposed two equations to estimate ϕ' and c' by using the initial void ratio, e_k, Equation 2.5 and 2.6.

$$c' = 430 * e^{-7.3e_k} \quad , kPa \tag{2.5}$$

$$\phi' = 35.3 - 9 * e_k \quad ,^{\circ} \tag{2.6}$$

More recently, these two set of equations were compared to another study conducted by SGI (Larsson, 2001). In this study, clay till samples were collected from a reference site located in Tornhill just north of Lund (Dueck, 1995). The author determined that the equations does not necessarily improve the simple assumptions used in Swedish practice, in which the ϕ' is 30° and c' is equal to 10% of the undrained shear strength, i.e. $0.1c_u$ (Larsson, 2001). Figure 2.1 and Figure 2.2 show the comparison between the measured data for effective cohesion and friction angle respectively with the calculated data from the two sets of equations by Jacobsen and Hartlén.

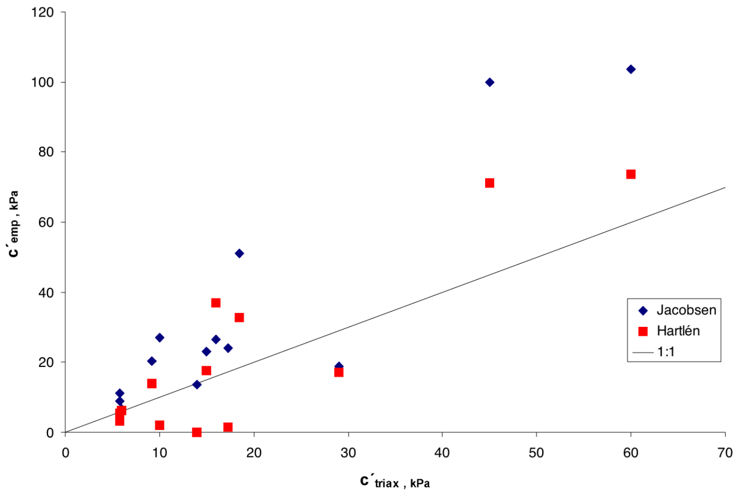

Figure 2.1: Comparison of effective cohesion between calculated and measured data (Larsson, 2001)

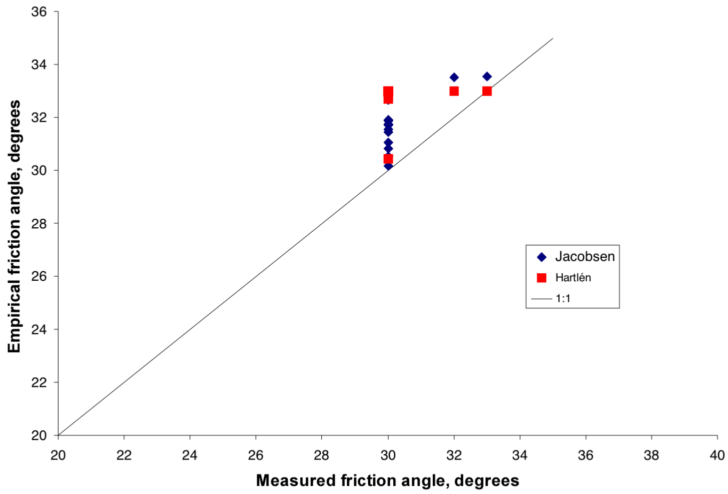

Figure 2.2: Comparison of effective friction angle between calculated and measured data (Larsson, 2001)

For the cohesion, the equation from Hartlén shows a random scatter whereas that of Jacobsen consistently overestimate the value. For the friction angle, the equation from Hartlén shows a consistently higher value than the assumed 30°, but since the equation is only valid for friction angle up to 33°, the constraint had to be applied. The equation from Jacobsen also consistently shows the the friction angle is higher, although not by much. Nevertheless, since the difference is minimal, it was suggested to keep the simple assumption of 30° and $0.1c_u$ for the effective friction angle and cohesion. However, according to feedback from the industry, these assumptions often lead to an overdimensioned structures, and thus there is a further need of have a deeper understanding of clay till behaviour in drained conditions and of a more accurate estimation of the effective strength parameters.

2.2 Scope of Study

This study sets out to further investigate the behaviour of clay till in drained conditions. This is done by conducting drained triaxial tests to minimise the need of interpretation from total stress parameters. Further, clay till is highly heterogeneous and well-graded. Thus, image analysis will be performed to visualise how the large inclusions in the sample can affect its behaviour.

3

Experimental Campaign

3.1 Site Selection

In this project, clay till samples are collected at a reference site located in Tornhill in north of Lund (see Figure 3.1). The site is chosen because it has been identied as a reference site for clay till which include previous studies done here (Dueck, 1995, Larsson, 2001). This allows this project to start with existing data which can be used to help verify findings in this study.

Figure 3.1: Location of clay till reference site in Tornhill

Two different types of clay tills are found in the site. The first 3m of the site consists of Baltic clay till. It is then followed by 3m thick transition layer consisting of Baltic clay till and Northeast clay till. Subsequently, Northeast clay till is then found below the transition layer up to 23m deep below the surface, see Figure 3.2

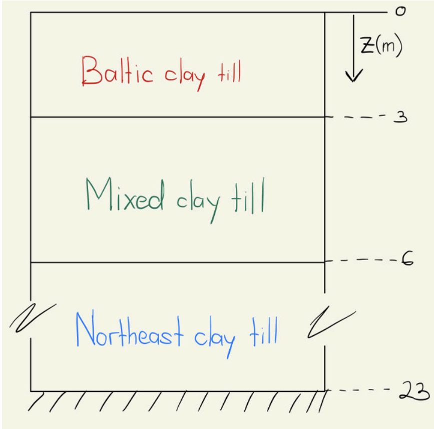

Figure 3.2: Soil profile in Tornhill

3.2 Samples Collection

Clay till sample was collected using an excavator to dig into the site and collect the soil. The soil was collected at two different depths, one at around 0.9m and the other at around 1.5m. Both clay tills are categorised as Baltic clay till. During the excavation, it was observed that the clay tills collected from the lower depth is wetter. This is in line with the information that the groundwater table is found at approximately 1m depth. As such, clay till collected from the lower depth will be used for the laboratory testing. Once collected, the samples are then stored in a refrigerator to maintain its moisture.

Some basic properties of Baltic clay till from previous studies are reported in Table 3.1. In this project, the bulk density and natural water content from the lower depth were investigated and they were found to be consistent with previous researches.

Table 3.1: Basic properties of Baltic clay till (Dueck, 1995)

Property	Unit	Baltic clay till
Bulk density	t/m^3	2,11
Natural water content	%	17,0
Liquid limit	%	32,0
Plastic limit	%	16,3
Degree of saturation	%	84,0
Clay content	%	35,0

3.3 In-situ Tests

Cone penetration tests (CPT) and dilatometer tests were planned in this project. However, due to unavailability of suitable tools, only CPT were conducted thus far. A total of five CPTs were conducted. As the focus was on Baltic clay till, each of the CPT were performed up to approximate 2m in depth.

Undrained shear strength of the soil can then be estimated from the CPT data using Equation 3.1. In this project, the value of N_{kt} is chosen to be 11 as recommended by Swedish Geotechnical Institute (Larsson and Åhnberg, 2003).

$$c_u = \frac{q_t - \sigma_{v0}}{N_{kt}} \tag{3.1}$$

where:

c_u = Undrained shear strength
q_t = tip resistance
N_{kt} = cone factor

A geophysical seismic survey was also conducted. Two parallel lines were laid as per Figure 3.3. The lines were 80m long and geophones were put along the line at a 1m spacing.

Figure 3.3: Geophysical seismic survey in Tornhill

3.4 Laboratory Tests

In this project, consolidated drained (CD) triaxial tests will be performed. CD is chosen because it is able to directly provide drained parameters of the sample. Details of the test including its setup will be described in Chapter 4.

3.5 Image Analysis

As the mechanical behaviour of clay till is highly dependent on the inclusions, it is important to further investigate their role. This will be done via image analysis using x-ray tomography. The details will be included in Chapter 6.

4

Triaxial Test Setup

This chapter discusses the experiment procedure used in this study. Firstly, the procedure to prepare the triaxial specimens is explained. Lastly, equipment and testing procedures will be described.

4.1 Sample Preparation Procedure

First, disturbed samples are taken out from storage, i.e., a refrigerator. Then an adequate amount of material is placed into a mould for compaction by layer. Compaction is performed with the help of a compactor (shown in Figure 4.1). The layers are about 30 mm thick to ensure that the sample is evenly compacted. Once the material is compacted, grooves are made on the surface so that the different layers mesh well with one another.

Figure 4.1: Compactor used for sample preparation

Once the sample is prepared, it is first weighed with the mould. Then, it is extruded out of the mould for testing and the mould is weighed to determine the weight of the sample.

4.2 Testing Procedure and Apparatus

4.2.1 Triaxial Test Setup

Tests were performed using a high-pressure triaxial test system in which both the confining pressure and the pore pressure were controlled by GDS Standard Digital Pressure Controllers. The triaxial cell and load frame are the same used previously in Holmén (2003). The triaxial cell is from Wykeham Farrance, and is capable to perform triaxial tests with sample diameters up to 100 mm and can withstand an internal pressure of 1,7 MPa. To avoid size effect on the sample, there is a need to ensure that the sample size used in the triaxial test is at least eight times larger than the largest particle found in the sample (Lade, 2016). This allows a sample of 100 mm to have inclusions with sizes up to approximately 12 mm in diameter without having significant size effect.

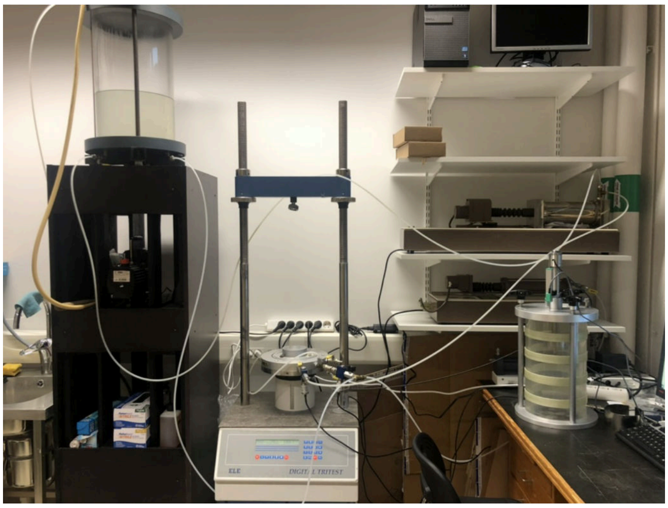

Figure 4.2: Triaxial test setup in LTH Geotechnical Laboratory

The load frame is from ELE international and is capable to withstand a force of 50 kN. Load cells up to 25 kN are used, which means that the setup can now achieve a σ_1 up to 3 MPa for samples with diameter of 100mm.

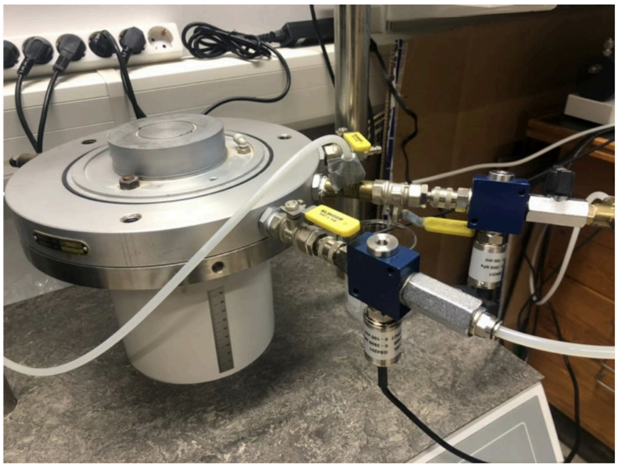

Figure 4.3: Triaxial base with 100 m pedestal and pressure transducers attached

Changes in pressure in the cell and within the specimen can be monitored using pressure transducers whereas changes in volume can be measured by monitoring the volume change in the GDS pressure controller that is controlling the back pressure. Within the specimen, pressure changes are controlled from both end of the sample to reduce the time taken for the sample to stabilise after a change in stress. time Upon testing, it was determined that a strain rate of 0,001 mm/min is suitable to account for the dissipation of excess pore water pressure generated during shearing. Axial displacements were measured using a linear potentiometric transducer. All the data is digitally recorded using by a computer system via a data logger and can be monitored in real time, see Figure 4.4.

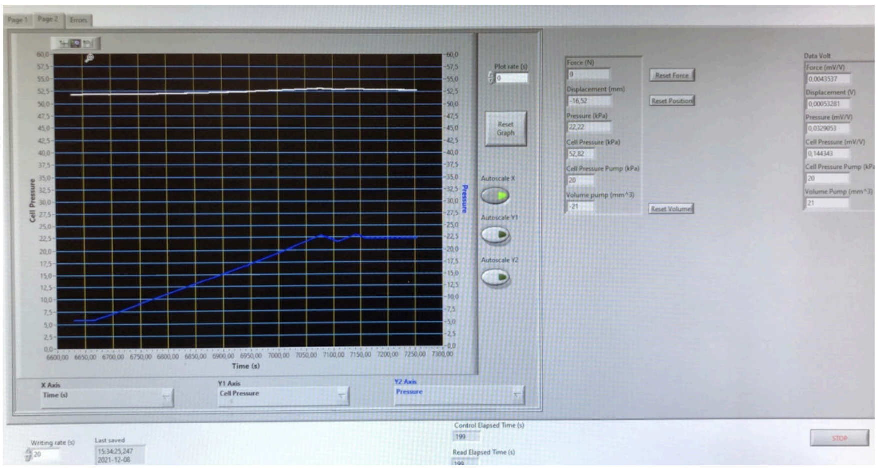

Figure 4.4: Screen capture of the LabView program used to log data

4.2.2 Methodology

All tests performed in this project is consolidated drained (CD) triaxial tests. First, the sample is consolidated to its preconsolidation stress. This was done at an effective stress of 500 kPa which is the preconsolidation pressure for the Baltic clay till found in Tornhill (Larsson, 2001). Once the consolidation is completed, indicated by a stabilisation of the excess pore water pressure and volume change, the sample is unloaded completely and dismounted from the cell frame for pre-mortem imaging by x-ray tomographic scan. Once the imaging is completed, the sample is loaded again, this time to the chosen effective stress. Once the sample is stable, shearing is commenced. Shearing is stopped once the peak force was observed or when it has plateaued, after which the sample is dismounted and scanned again for a post-mortem imaging. While normally the test is continued further until approximately 5% strain after the peak or plateau, in this case only an excess 2-3 % strain was kept. The reason is because a post-mortem imaging will be performed on the sample, and huge deformation is undesirable.

A total of four CD tests were conducted on 100 mm diameter samples. As one of the objectives of the study is to obtain the effective cohesion and friction angle, the initial effective stress, σ'_3 was varied in the tests. Table4.1 shows the chosen confining pressure, σ'_3, for the tested samples. For all tests, a saturation check is first performed on the sample by checking that the Skempton B-value is at least 0,9. In all the tests performed, the B-value constantly measured above this value. To accelerate drainage, side drainage and filter papers at both ends of the specimens were used.

Table 4.1: Table of CD tests conducted

ID	σ'_3 (kPa)
TC01	40
TC02	40
TC03	80
TC04	20

5

Results

In this chapter the results from in-situ and triaxial CD tests will be presented.

5.1 In-situ Tests

The undrained shear strength obtained from the CPT is shown in Figure 5.1. Generally, the undrained shear strength starts high. It then decreases in value at around 0,4 m depth and then it slowly increases with depth. The same behaviour was observed in Dueck (1995). To approximate the undrained shear strength at 1,5 m depth, which was where the samples for the laboratory tests were collected, the average undrained shear strength from 1,4 m to 1,6 m depth was used. This gives an average undrained shear strength of 350 kPa. Data from CPTR4 was not used as the CPT stops before 1,6 m depth.

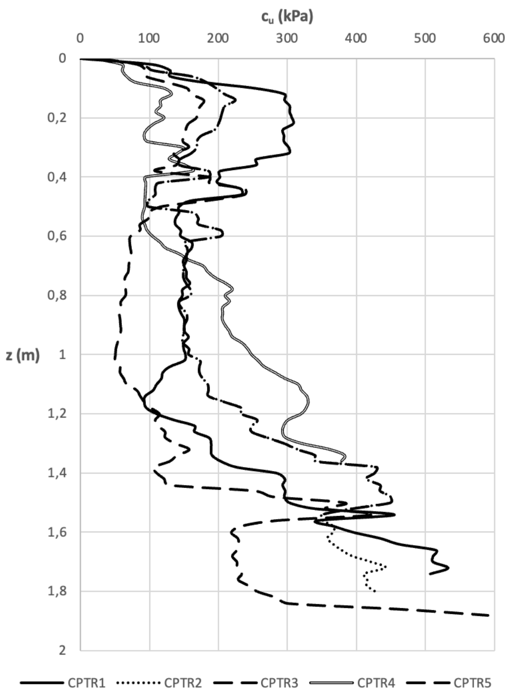

Figure 5.1: Undrained shear strength from CPT

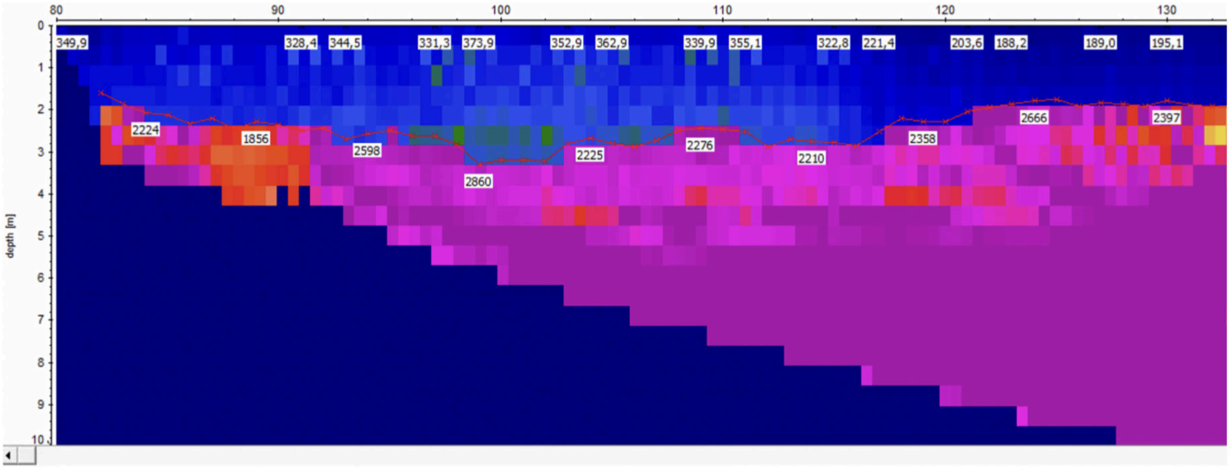

Figure 5.2: Shear wave velocity from seismic survey

5.2 Triaxial Test

Figures 5.3 and 5.4 show the Mohr's circles and the p'-q stress space diagram obtained from the CD triaxial tests respectively. Results from sample TC01 have been omitted as the results show abnormal stress path and very low σ_1' at failure. One possible reason for the abnormality is that channeling might have occurred in the sample, which caused drainage to occur in a specific path instead of having the sample drain homogeneously.

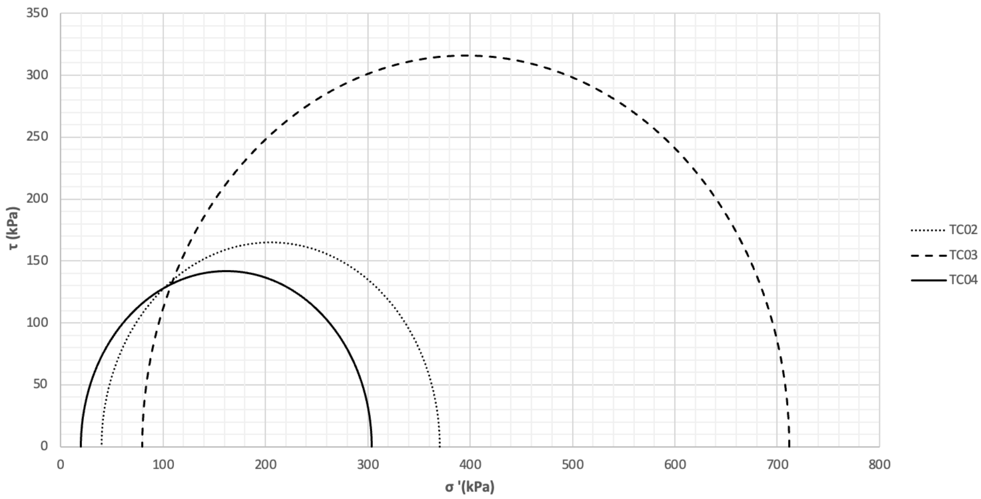

Figure 5.3: Mohr's circle from CD triaxial tests

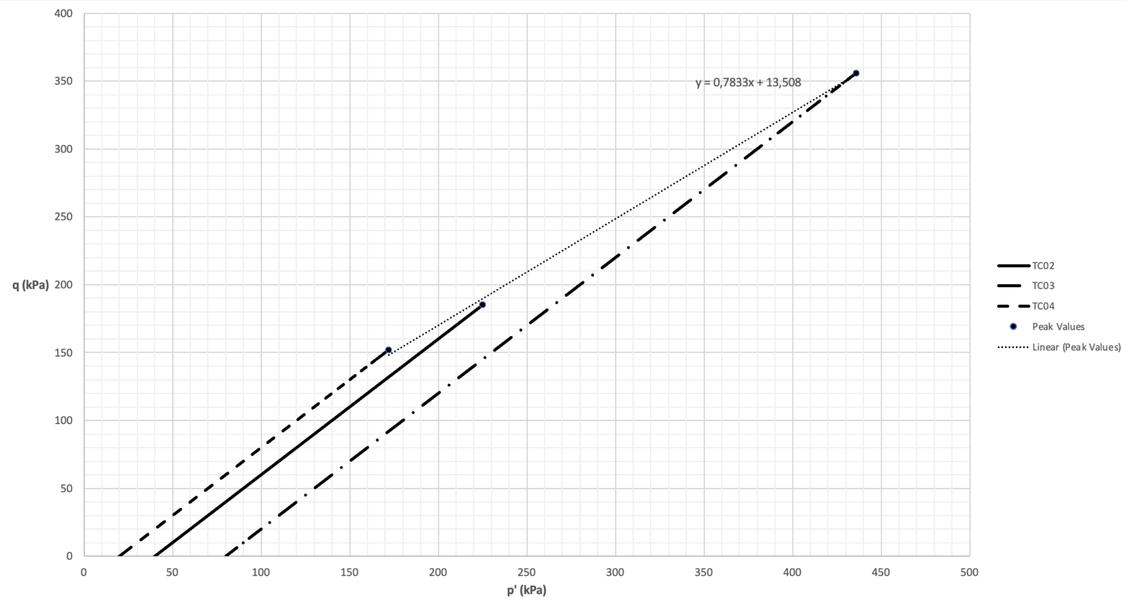

Figure 5.4: p'-q stress space diagram from CD triaxial tests

From the p'-q stress space diagram, the peak value from the stress path of each of the samples are chosen to form a trendline which serves as the failure envelope. The properties of this trendline can then be used to derive the effective cohesion and friction angle, c' and ϕ' respectively. The slope angle of the envelope, β can be converted into ϕ' where $sin\phi' = tan\beta$. On the other hand, the y-intercept, d, can be converted into c' where $c' = \frac{d}{cos\phi}$. From Figure 5.4, a value of 51° and 21,7 kPa for ϕ' and c' respectively is obtained.

Alternatively, another p'-q stress space diagram was obtained by further excluding results from TC03, see Figure 5.5. With this data, a value of 38° and 57,3 kPa for ϕ' and c' respectively is obtained instead.

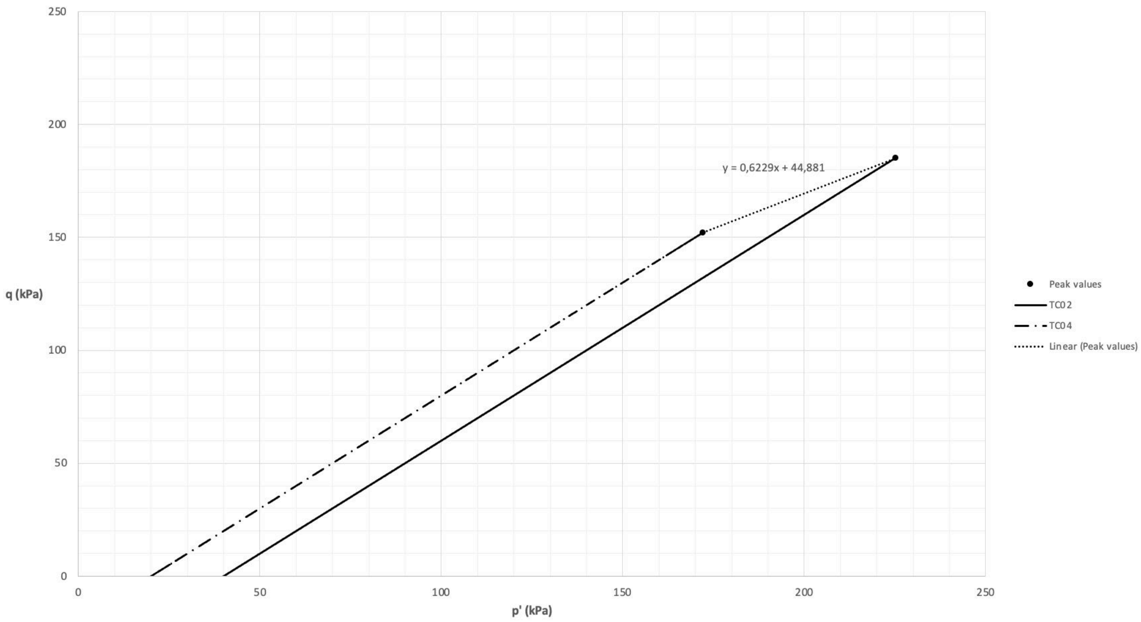

Figure 5.5: p'-q stress space diagram from CD triaxial tests excluding TC03

6

Image Analysis

In this chapter, image analysis will be discussed. At first, the theory of the method, both image acquisition and image processing, will be described. Then, the methodology implemented in this projected will be presented. Lastly, the results will be shown.

6.1 Theory

6.1.1 X-ray Tomography

X-ray tomography (XRT) is obtained by first acquiring a 2D projection of the sample by shooting rays of x-rays through the sample. The 2D projection, also known as a radiogram, is based on the attenuation of the x-rays from transmitting through the sample. The attenuation can be calculated based on Beer-Lambert attenuation law which states that the attenuation is largely controlled by the density and the size of the object. Multiple 2D projections are then taken around the sample either by rotating the sample or the x-ray source.

Multiple projections are obtained by either moving the x-ray source or the sample. In the medical field, it is more common to move the x-ray source. However, in the industrial and synchrotron set-up, it can be costly or impossible to move the x-ray source. Instead, the sample is rotated. Once multiple projections are acquired, the slices of a 3D volume can be reconstructed. This can be done algebraically, which requires less projections. However, the computation is intensive and was not available in the early days. Instead, the slices are reconstructed by using backprojection using an inverse Radon transform.

For optimal reconstruction, it is best to use a synchrotron. However, it is only applicable for small specimen size in the magnitude of mm. Furthermore, they are difficult to access. On the other hand, using an x-ray tube is more accessible and could be more beneficial to scan larger samples.

In experimental geomechanics, XRT is often performed pre- and post-mortem of an experiment involving compression of samples. The images can provide information on how the grains have changed, moved, or crushed depending on the stress applied. XRT can also be performed in-situ. This way, evolution of the grains could be identified with respect to the increasing loading. This require, however, special equipment that can be place inside the tomograph.

6.1.2 Digital Image Correlation

Digital Image Correlation (DIC) is a complementary, non-contact technique which can provide a full-field measurement of displacement on either 2D or 3D surfaces, or volumes depending on the type of DIC. In other fields, DIC is also called Partical Image Velocimetry (PIV). In principle, DIC is performed by comparing two images, the first being the reference image and the second being the target image. A grid is created based on the reference image which covers the region of interest of the sample. In each node of the grid, a small subset of the image with known location from the reference image, also known as a motif, is first taken. The new location of the motif in the target image is then determined. This is done by first placing the motif in the target image in the same location as the reference image. The motif is then moved around step-wise within a search window of a specified size. For every movement, a correlation coefficient (CC) is calculated to determine how good of a fit the new motif is compared to the original. The position with the highest CC is then selected as the final movement of the motif from the reference to the target image. In its most simplest form, only translational movement is checked in the target image. However, more complicated programs could look into rotational and transformation as well. After all the movement for all motifs have been identified, DIC provides a displacement field for all points in the grid. The field can then be transformed into strain field that can be used for further studies on localised phenomenon such as locating and quantifying localised strain. If more than two images are available during testing, DIC could also provide the evolution of the displacement field as the test progresses, which gives further information on when the localised strain starts to form. This information could be used to develop a more appropriate model at different stages of loading.

To get started with DIC, first one would need images of the sample that were taken concurrently as the test is ongoing or pre- and post-mortem. The most common method to obtain the images is via photography, having a camera take a picture of the sample at a set time interval. However, other form of imaging such as x-ray tomography can also be used. These images will act as the canvas for DIC, in which the program will track subsets of the reference image and find their location in the next one. Depending on the available type of images different DIC analysis can be performed. 2D-DIC can be obtained from 2D images such as photographies. In this case, it is often required that the sample can not deform in the direction perpendicular to the photograed surface. To carry out 3D-surface DIC it is required that al least 2 picture of the sample are acquired simultaneously from different angles. This will capture the 3D mouvements of the surface of the sample. Finally, if 3D volumes of the sample are available, 3D volumentric DIC, also known as Digital Volume Correlation (DVC), can be performed. This will provide the displacement even of the internal point of the sample.

The way the DIC analysis is performed can also be different in terms of the way each nodes are treated. One way is to provide no restriction in terms of how the nodes move with respect to adjacent nodes. This will allow for a freer DIC analyis, which can lead to a shorter processing time. This type of DIC is also known as local DIC. On the other hand, the nodes can also be restricted on how they move based on the adjacent nodes. In other words, the degree of freedom each node has is dependent on the setup of which adjacent nodes control the movement. This type of DIC is known as global DIC. While global DIC is expected to provide a more representative displacement field, it will also take more time to perform the computation.

6.2 Methodology

In this project, for each of the triaxial samples, two XRT were acquired. The first after the consolidation stage and just before shearing (pre-mortem). This was done by dismounting the sample from the triaxial cell. The sample is then transported to the imaging lab, 4D Imaging Lab, located within the division of Solid Mechanics in Lund University, see Figure 6.1. The imaging process takes approximately one hour, after which the sample is transported back to LTH Geotechnical Laboratory where it is re-mounted on the triaxial cell. The sample is then loaded to the chosen initial effective stress and shearing starts after the pressure and volume change is stable. After shearing is completed, the sample is then brought to the imaging lab once again for another round of imaging (post-mortem).

Figure 6.1: Image acquisition via XRT in 4D Imaging Lab

For analysis, DVC was implemented by using the pre- and post-mortem as the initial and final condition of the sample. Both shear and volumetric strain evolution within the sample can be obtained and visualised to have a better understanding on how they develop.

6.3 Results

Figure 6.2 and Figure 6.3 show two horizontal and one vertical slices from the same sample obtained using x-ray tomography. The slices show that the inclusions can be clearly identified from the clay matrix due to the different density and that their size and distribution is scattered randomly within the sample.

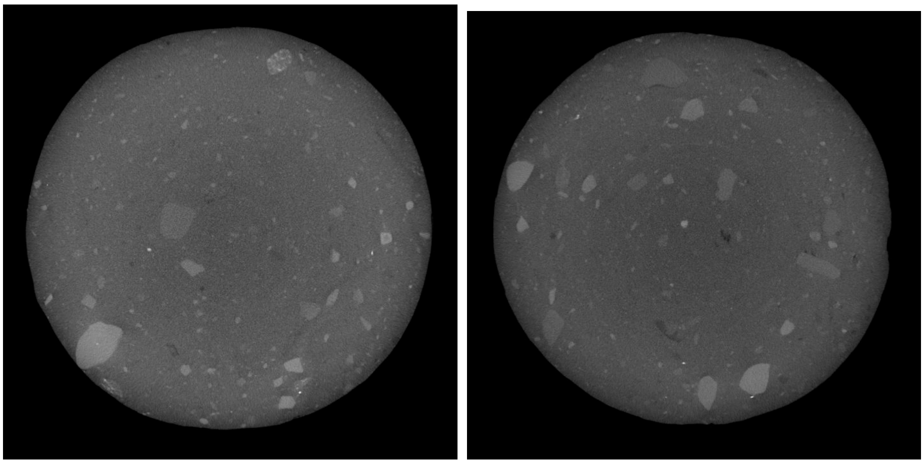

Figure 6.2: Sample slices from TC02 (Post-mortem)[Plan View]

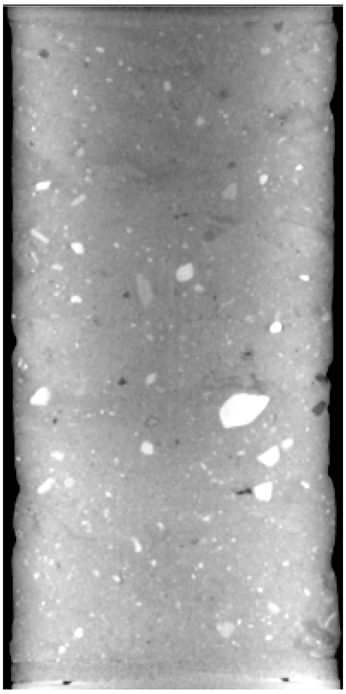

Figure 6.3: Cross Section of TC02 (Post-mortem) using XRT

Figure 6.4 shows the shear and volumetric strain in the middle vertical slice of the sample after DVC was conducted. In the shear strain analysis, black colour indicates no strain whereas bright pink indicates high shear strain. On the volumetric strain, white indicates no strain whereas red indicates zones experiencing dilation and blue zones experiencing compaction.

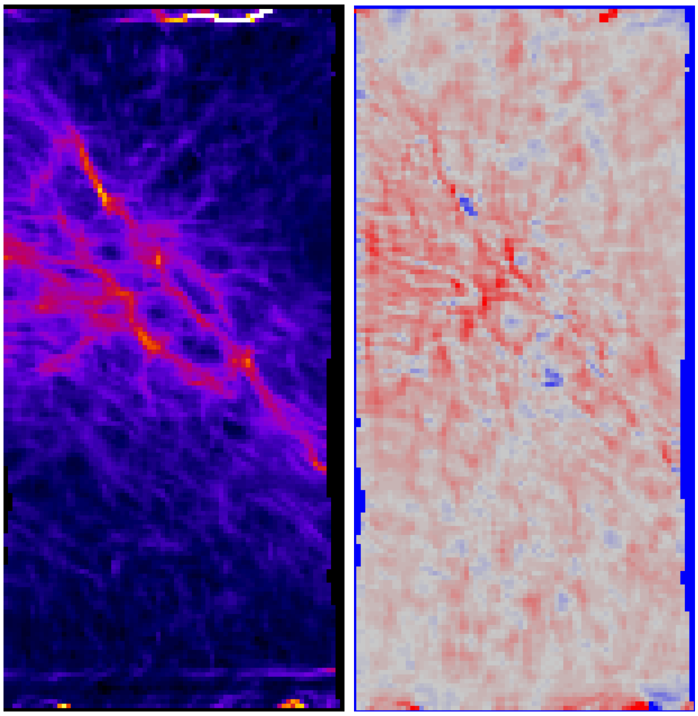

(a) **(b)**

Figure 6.4: (a) Shear and (b) volumetric strain of TC02. In (a), black colour indicates no strain whereas bright pink represents high shear strain. In (b), white indicates no strain, whereas red and blue represents dilation and compactionr respectively.

7
Discussions

Discussion arising from the results obtained in Chapter 5 and Chapter 6 will be held here. First, the implications of the findings from both the CPT and triaxial tests will be reviewed, alongside their drawbacks. Then, results from the XRT and the image processing will be discussed.

7.1 Geotechnical Tests

In general, the undrained shear strength obtained from the CPT falls within the range obtained from previous CPT results which were found to be between 200 to 400 kPa (Dueck, 1995, Larsson, 2001). The large range is due to the heterogeneity of the soil, coupled with the presence of inclusions that are scattered which can cause the undrained shear strength to have a large variation.

With regards to the triaxial tests, two sets of drained parameters, which are effective friction angle and cohesion, were obtained. The reason behind the second set, which was obtained by omitting TC03, is due to the seemingly large Mohr's circle obtained from the test (see Figure 5.3). Furthermore, the results from these tests are not definitive due to the low amount of tests. As such, more tests will be required in order to come up with a more definitive finding.

In the industry, it is common to assume an effective cohesion c' to be 10% of the undrained shear strength. Using the value obtained from the CPT, this gives an estimated effective cohesion of approximately 35 kPa. Further, the effective friction angle ϕ' is assumed to be a constant 30°. On the other hand, the two sets of values obtained from the triaxial tests are 21,7 kPa and 51°, and 57,3 kPa and 38°. While the triaxial tests were conducted on remoulded samples, no differences are to be expected based on previous report (Hartlén, 1974). Furthermore, the triaxial test results can be deemed to not be fully conclusive due to the low amount of tests. Nevertheless, the findings have shown that the material exhibits consistently higher effective friction angle. In one set of the results, the cohesion is also higher when compared to the values obtained empirically in the industry. This indicates that the designs are potentially over-conservative which can unnecessarily increase the cost of the construction.

7.2 Image Analysis

Based on Figure 6.1, presence of beam hardening was observed. Beam hardening is an artifact produced during the image analysis which cause the perception that the sample is denser on the outside than on the inside. This phenomena is more evident when the contrast of the image is further increased (see Figure 7.1). However, whether this phenomena is actually beam hardening is unclear. One way to reduce beam hardening effect while imaging is to use filters during the imaging process. This was implemented, only to results in minimal improvement. Alternatively, it is possible that the sample is actually denser on the outer edge. One hypothesis as how this could occur is due to the compaction process during sample preparation. When vertical force was applied by the compactor (see Figure 4.1), the soil being compacted is being pushed to the edge and then upwards where there is a small gap for the excess soil to escape. This movement may cause the edges of the sample to be more well-packed.

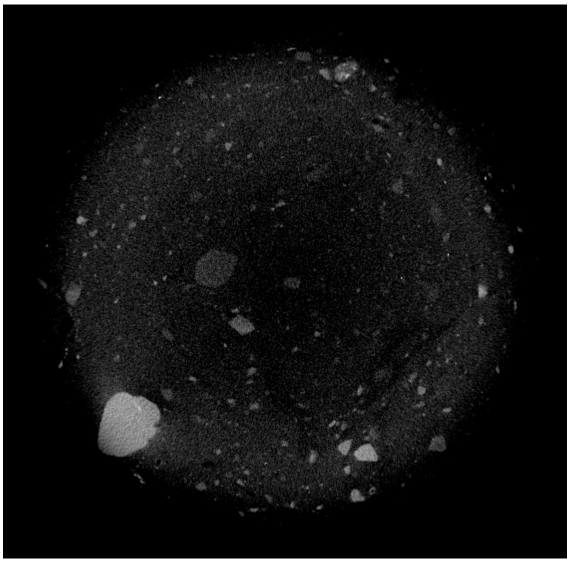

Figure 7.1: Example of Beam Hardening

In general, a clay sample will exhibit a singular major shear band, see Figure 7.2. However, in the clay till sample, interestingly there are at least 2 shear bands, each with a different angle. When the shear strain and x-ray images are overlaid on top of each other, it becomes clear that the shear band splits because of the inclusions, see Figure 7.3. As the inclusions are very stiff, a singular shear band could not be formed. Instead, it would need to skirt around the inclusions, resulting in a more complex shear strain localisation. More complex strain paths lead, in turn, to higher strength.

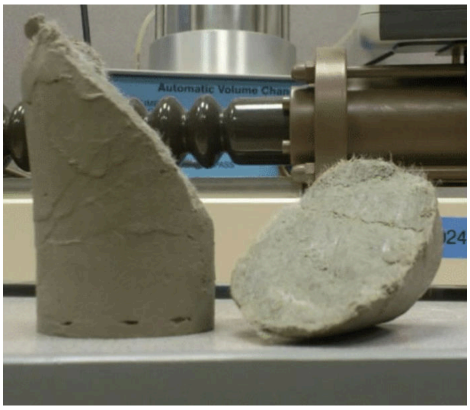

Figure 7.2: Typical behaviour of clay after shearing (Armediaz, 2015)

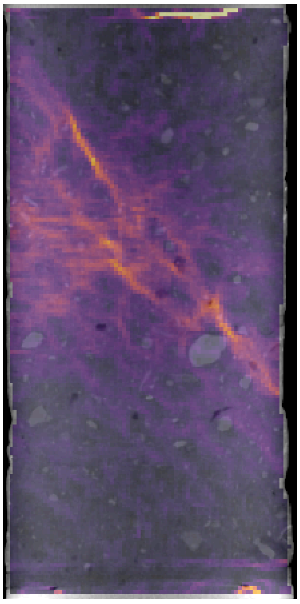

Figure 7.3: Overlaid image of x-ray and shear strain

It was also observed from the volumetric strain analysis that the sample seems to be dilating everywhere, and not only close to the shear band as it would be expected (see Figure 6.4b). One possible reason to this phenomena is that as the sample was unloaded after the preconsolidation phase, insufficient time was provided for the sample to be stabilised before the first scan. As such, the pre-mortem image shows the state of the sample where it is still undergoing dilation.

8
Conclusions & Recommendations

This study sets out to determine if the current empirical relationships are accurate in estimating to estimate the drained properties of clay till. The results are summarised in the following section. A proposal on future works is also provided.

8.1 Main Findings

CPT and consolidated drained triaxial tests were conducted on clay till samples collected in Tornhill, Lund. The drained properties obtained from the triaxial tests are then compared to the empirical relationship used in the industry. It was observed that the values from the triaxial tests indicate that the clay till samples are indeed stronger than what empirical formulae suggest. Nevertheless, since there are only a few triaxial tests conducted, this conclusion is not definitive.

Imaging is then performed on the sample to provide a better understanding of how the samples behave under shearing. The results show that the samples experience a complex behaviour with regards to the formation of the shear band due to the presence of inclusions which are scattered within the sample.

8.2 Proposals on Future Works

Firstly, to obtain a more definitive conclusion, more consolidated drained tests need to be conducted. Furthermore, to provide a more holistic, representative conclusion, clay till samples need to be collected from different sites.

The triaxial tests will also need to be coupled with a more thorough image analysis. This is proposed via performing imaging during the triaxial test. Currently, tomographies are only acquired before and after shearing. More imaging can be taken in stages as the the triaxial test is ongoing, allowing more insight on how the strain localisation evolve during shearing. This requires the design of a portable triaxial cell that can be placed inside the tomograph. Such a design is currently ongoing.

Further study is also suggested on how the inclusions in clay till can affect the drained properties. The amount, size, ans shape of the inclusions in clay samples can be varied to investigate how these factors influence the mechanical behaviour of the material.

Bibliography

Armediaz, Y. (2015). Pre-yielding behaviour of fibre-reinforced cement-treated singapore marine clay. *Bachelor's Thesis*.

Dueck, A. (1995). *Reference site for clay till*.

Hartlén, J. (1974). Skånska moränlerors hållfasthets-och bärighetsegenskaper:[the geotechnical parameters of strength and bearing capacity of boulders clays from the southwest part of sweden].

Holmén, M. (2003). *Advanced triaxial testing of clay till*. Lund University.

Jacobsen, M. (1970). Strength and deformation properties of preconsolidated moraine clay. In *Bulletin no. 27* (pp. 21–45). The Danish Geotechnical Institute.

Lade, P. V. (2016). *Triaxial testing of soils*. John Wiley & Sons.

Larsson, R. (2001). *Investigations and load tests in clay till. results from a series of investigations and load tests in the test field at tornhill outside lund in southern sweden* (tech. rep. No. 59).

Larsson, R., & Åhnberg, H. (2003). Utvärdering av skjuvhållfasthet och förkonsolideringstryck från vingförsök, cpt-sondering och dilatometerförsök.